International Journal of Theoretical Physics, Vol. 37, No. 12, 1998

Universal Dynamical Computation in Multidimensional Excitable Lattices

Andrew Adamatzky[1]

Received

We study two- and three-dimensional lattices nodes of which take three states: rest, eccited, and refractory, and deterministically update their states in discrete time depending on the number of excited closest neighbors. Every resting node is excited if exactly 2 of its 8 (in two-dimensional lattice) or exactly 4 of its 26 (in three-dimensional lattice) closest neighbors are excited. A node changes its excited state into the refractory state and its refractory state into the rest state unconditionally. We prove that such lattices are the minimal models of lattice excitation that exhibit bounded movable patterns of self-localized excitation (particle-like waves). The minimal, compact, stable, indivisible, and capable of nonstop movement particle-like waves represent quanta of information. Exploring all possible binary collisions between particle-like waves, we construct the catalogue of the logical gates that are realized in the excitable lattices. The space and time complexity of the logical operations is evaluated and the possible realizations of the registers, counters, and reflectors are discussed. The place of the excitable lattices in the hierarchy of computation universal models and their high affinity to real-life analogues affirm that excitable lattices may be the minimal models of real-like dynamical universal computation.

1. INTRODUCTION

Computational universality implies the ability to compute any logical function. To validate the computation universality of some abstract or real physical, chemical, or biological system we need to construct functionally complete system of Boolean functions, e.g., $\langle \bar{x}, x \wedge y \rangle$ or $\langle \bar{x}, x \vee y \rangle$. Given some physical, chemical, or biological system, to prove its computational universality, we have to represent (i) quanta of information (e.g., True and

[1] Intelligent Autonomous Systems Lab, University of the West of England, Bristol BS16 1QY, United Kingdom; e-mail: ai-Andrew.Adamatzky@uwe.ac.uk.

0020-7748/98/1200-306 9$15.00/0

False values of the Boolean variables), (ii) routes of information transmission, and (iii) logical gates where quanta of information are processed in the states of the given system.

The standard method of stationary computation (computation with stationary architectures) utilizes embedding of the entire architecture of the Boolean circuit into the given system in such a manner that wires, gates, etc., are presented in the stationary states of the system (namely in the absorbed states of the elementary units) and do not change their position with time [12, 49, 51, 56, 66].

The dynamical computation is an original nonstandard and widely accepted method. It assumes that autonomous signals travel in space and perform computation by colliding with other traveling signals. There are no specially determined wires; however, we can use mirrors to specify trajectories of the signal [45].

The billiard ball model [45] and the glider computation in the game of Life [15] are basic models of the contemporary theory of dynamical computation, particularly in cellular-automata models of natural systems.

Fredkin and Toffoli [45] were probably the first to prove that there is no need to keep the computer architecture stationary and unchanging: everything can move, collide, and compute by colliding. The discovery of gliders and glider guns in the game of Life led to the possibility of simulating universal logical gates via collisions between gliders [15] and other self-localized movable patterns [24, 25, 34].

Whereas physics-based universal computation has been evolving toward the design of interaction gates with Toffoli–Fredkin ideology, a new direction in natural computing emerged from the study of nonlinear homogeneous chemical media. This is reaction-diffusion computing. The discovery of light-sensitive modification of the Belousov–Zhabotinsky reaction by Kuhnert [54] and its application to image processing [55] were the starting points for the design of working prototypes of distributed chemical computers [64, 65, 75, 76, 79, 8].

All reaction-diffusion algorithms are deeply intuitive: the data are represented by the concentrations of reagents spatially distributed in chemical solutions or films with immobilized reagents. The sites of the chemical space where the data-reagents are initially applied generate concentration waves that spread, collide with one another, and produce a precipitate or dissipative structures of stationary concentrations of the reagents. The distribution of precipitate represents the results of the computation. All chemical processors with homogeneous computational space are highly specialized. They are designed to solve only one problem, e.g., image enhancement or contouring [64], approximation of a Voronoi diagram [79], or search for the exit out of a labyrinth [75, 8].

However, the recent results of Blittersdorf *et al.*, [18], Tóth and Showalter [80], and Steinbock *et al.*, [76] show that logical gates can be realized when computational space is structured. The chemical waves travel inside the tubes and interact one with another in the tube junctions. So, the space is highly inhomogeneous. The wires are predetermined and there is little difference between such chemical models and logical operations realized in the living axons or dendrites.

Is it possible to make the two- and three-dimensional reaction-diffusion processors *dynamically computationally universal*? To prove the answer is yes, we use a reduced version of reaction-diffusion systems: excitable lattices. We demonstrate that excitable lattices exhibit a wide range of the movable self-localized patterns of excitation (particle-like waves) and that universal logical gates are realized at the sites of collision between these mobile patterns. Keeping in mind that our models of excitation are far from the disappointing reality, we decided to play all possible scenarios of the collisions. That is, we investigate almost all possible binary and ternary collisions of the particle-like waves in two- and three-dimensional excitable lattices and compile a catalog of the interaction gates that are realized as the result of the collisions. Most of the gates are proved to be logically universal and so our simple models of lattice excitation are universal computers. The complexity of the models is analyzed and comparison with existing cellular-automata models of universal computation is provided.

Various models of universal computation in automata networks are discussed in Section 2. The basic model of lattice excitation is defined in Section 3. Section 4 introduces and characterizes multidimensional particle-like waves. The generators of the particle-like waves, or the so-called particle guns, are investigated in Section 5. Section 6 presents a catalog of the interaction gates. Possible ways to construct counters and registers are discussed in Section 7. In Section 8 we compare the complexity of universal computing in the excitable lattice and the game of Life. Possible real-life candidates for the role of dynamical universal computers are discussed in Section 9. Potential techniques for the discovery of universal computers are discussed in Section 10.

2. UNIVERSAL COMPUTATIONS IN AUTOMATA NETWORKS AND MODELS OF NATURAL SYSTEMS

Generally speaking, a universal computer is a device that implements computable recursive functions and composition rules, i.e., null function, successor function, projection operation, function composition, primitive recursion. Fisher [40] and Mazoyer [56, 66] proved that even a one-dimensional cellular automaton makes arithmetic computations and simulates

recursive functions. So, such a automaton is universal. However, the signals that carry information and the proper cell states are separated in these models; the static architecture of the computer is really embedded into the configurations of the cellular automaton.

An entirely new field of particle models of computation was developed by Steiglitz, Squier, *et al.*, [62, 74, 70–73]. Their *particle machines* are one-dimensional, but truly *dynamical* computing devices: the particles propagate and collide, and implement computation as the result of collisions. In the particle models the units of information are encoded in the vector states of the particles.

An abstract machine is called universal (actually simulation universal) if it simulates the univeral Turing machine. Thus, e.g., the cellular automaton is universal if it simulates the Turing machine and any other cellular automaton (see, e.g., ref. 59).

Finally, there is the commonsense notion that a universal computer is *one that can be programmed to perform any digital computation* [14]. A series of physical models have been considered as universal computers: hard-sphere gas, lattice gas, systems of partial differential equations, and single particles moving in the a room with plane and parabolic mirrors [14].

In the present paper we assume that a computing device is universal if it computes any Boolean function (function of the algebra of logic) presented in the form f: $\{0, 1\}^k \to \{0, 1\}$.

From the basics of Boolean algebra we know that every Boolean function can be represented in disjunctive normal form:

$$f(x_1, \ldots, x_k) = \bigvee_{\substack{(\sigma_1, \ldots, \sigma_k) \\ f(\sigma_1, \ldots, \sigma_k)=1}} x_1^{\sigma_1} \wedge \cdots x_k^{\sigma_k}$$

The $f(x_1, \ldots, x_k) \equiv 0$ is represented by $f(x_1, \ldots, x_k) \equiv x_1 \wedge \overline{x_1}$. Therefore every Boolean function is represented via negation, conjunction, or disjunction. That is, e.g., the systems $\{\overline{x}, x_1 \wedge x_2, x_1 \vee x_2\}$ and $\{\overline{x}, x_1 \wedge x_2\}$ are functionally complete.

2.1. Neural and Reaction-Diffusion Networks

Neural and reaction-diffusion networks (in their purely abstract form) have been proven to be universal. The simulation universality of a neuron-like network has been demonstrated by Siegelman and Sontag [69]: every neuron of the network has a linear combination of inputs and a saturated linear threshold function. Assuming that universality of the neural networks is proved, Goles and Matamala [51] show that a three-state automata network is universal because it simulates any neural network. The sandpile model (which is discussed below) is a more realistic species of reaction-diffusion

models, so the proof of universality of the one-dimensional reaction-diffusion medium can be accepted in general via the proof of universality of the sandpile model [49].

The continuous and hybrid systems constitute another class of universal computers. One of the first substantiated claims on the universality of partial differential equations with continuous time was that of Omohundro [60], who proved that any two-dimensional cellular automaton with (8 + 1)-cell neighborhood is simulated by a system of ten coupled partial differential equations. The cellular automaton in its turn simulates, a Turing machine. Therefore, that system of differential equations is universal.

As a corollary to the simulation of discrete systems by continuous and hybrid systems (which are obviously a superclass of the neural networks), Branicky [21] showed that a Turing machine is simulated by ordinary differential equations in three-dimensional real-valued space. Elaborating the Korian-Cosnard-Garzon idea [53] on the simulation of a universal Turing machine by a two-dimensional piecewise linear iterated function, Orponen and Matamala [61] confirmed that one- and two-dimensional gridlike networks of coupled oscillators simulate a Turing machine, and therefore arrays of the coupled oscillators are universal.

2.2. Sandpile Model

The sandpile model of Goles and Margenstern [49] is among the most attractive models of universal computation. It originates from the physical sandpile model [10], combinatorial games with discs and balls [9], and chip firing games [50, 16]. The sandpile model configurationally simulates logical gates and registers.

2.3. Billiard Ball Model

The billiard ball model, with its *binary "signals" traveling on the grid and interacting with one another* [45] is probably the most famous model of universal physical computation. Created by Fredkin and Toffoli [45] in the context of conservative logic, the model is based mainly on idealized elastic collisions between balls and unmoveable reflectors. The balls of finite diameter move with constant velocity along straight trajectories on a planar grid. A bit of information is represented by the presence or absence of a ball at a given time at a given site. The routes of the information flow are represented by the trajectories of the balls (crossover is trivially prevented) and routing is implemented by the orientations (initial configuration) of the reflectors.

The elementary interaction logical gate of the billiard ball model that computes $\bar{x}y$, $x\bar{y}$, xy (we write xy for $x \wedge y$) functions is shown in Fig. 1A, with its ball representation Fig. 1B. From the elementary gates and the mirrors (that reflect the balls) the switch and the so-called Fredkin (conservative) gates are constructed. One practical application of the Fredkin gate is found in magnetic-bubble logic and conservative logical circuits [24]. Also, Chau and Wilczek [25] designed a Fredkin gate using a sequence of six 2-body quantum gates. Some recent results related to the universality of the billiard ball model in the sense of Margolus neighborhood are presented in ref. 34.

2.4. Game of Life

The *game of Life* is one of the first cellular-automata models proved to be dynamically computation universal [15]. This is a two-dimensional automaton with 8-cell neighborhood and binary cell state set. The Life rule is attractively simple. Every cell in the 1-state does not change its state if it has exactly two or three neighbors in the 1-state. The cell switches from 0-state to 1-state when there are exactly two neighbors in the 1-state. The self-localized oscillating translating patterns—gliders and spaceships—and generators of the movable patterns—glider guns—usually emerge in the space-time evolution of the game of Life automaton that starts from the random initial configuration. The gliders can be considered as the analogs of balls, which represent, transmit, and process information. The gliders do not collide elastically. Both gliders disappear as the result of a collision and the interaction gate has not four, but two outputs, as in Fig. 2. Therefore, the only $\bar{x}y$ and $x\bar{y}$ functions can be computed in single collision of two gliders.

The universality of the game of Life is proved in ref. 15 by the construction of universal logical functions via collisions of glider streams. If the distances between neighboring gliders in a stream are fixed, then every glider will represent 1, or Truth, and the absence of a glider — 0, or False. If two gliders collide with each other, they annihilate. The glider streams from the glider gun can be considered as 1 constant. Therefore, a $\bar{x}$ gate is constructed

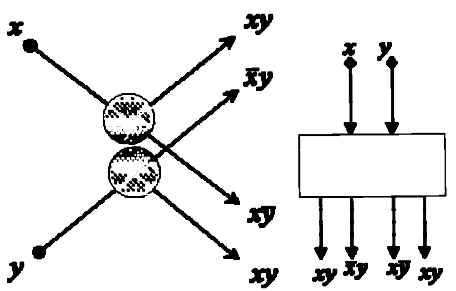

Fig. 1. Billiard ball interaction gate.

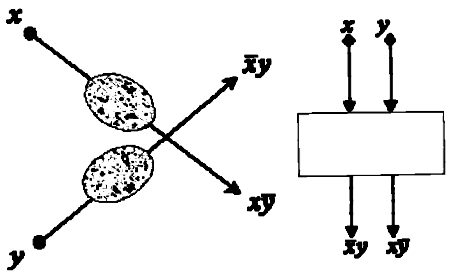

Fig. 2. Glider interaction gate.

in the following way: a data stream x of gliders runs across a stream of gliders generated by a glider gun. When a glider from the data stream collides with a glider from the glider gun it annihiliates. If it does not meet a glider from the glider gun it continues to move undisturbed. As a result of the stream interaction, we receive the stream $\bar{x}$ of gliders and holes that represents the result of the computation. Combining the glider streams from the glider gun with the data streams x and y, we can produce $x \vee y$ and xy streams.

2.5. Life without Death

Griffeath and Moore [48] designed a model that realizes interaction logical gates in the collision and interaction of wormlike patterns, so-called ladders, which grow in the evolution of two-dimensional cellular automaton with 8-cell neighborhood and binary cell state set. Every cell of the automaton takes the 0- or 1-state and updates its state by the following simple rule: A 0-state cell takes the 1-state if exactly three of its neighbors are in 1-states. The 1-state is absorbing. The trajectories of the billiard balls are simulated by quasi-one-dimensional ladders that grow in one of the four directions, i.e., along the columns or rows of the cellular array. The ladders can be turned, blocked, and delayed. Immortality is the only but significant disadvantage of the model: the trajectories of the ladders cannot intersect each other.

3. THE MODEL OF AN EXCITABLE LATTICE

Every cell of the discrete lattice **L** takes three states: . (rest), + (excited), and − (refractory), and changes its states deterministically in discrete time depending on the states of its closest neighbors. Every cell x of **L** has 8-cell neighborhood in a two-dimensional lattice and 26-cell neighborhood in a three-dimensional lattice, i.e., a neighborhood of cell x includes all the cells being at the distance 1 (in L_∞ metric) from x and does not include the cell x itself.

The rest cell becomes excited if exactly 2 (in the two-dimensional lattice) or 4 (in the three-dimensional lattice) of its neighbors are excited and passes

from the excited state to the refractory state and from the refractory state to the rest state unconditionally, i.e., independently on the states of its neighbors.

The cellular-automata model $\mathbf{M}^+$ of the lattice excitation is the tuple $\langle \mathbf{L}, \mathbf{Q}, u, f \rangle$, where $\mathbf{L}$ is a two- or three-dimensional array of cells, $\mathbf{Q}$ is a set of cell states, $\mathbf{Q} = \{., +, -\}$, u: $\mathbf{L}^k \to \mathbf{L}$ is a neighborhood function, which assigns k different cells of $\mathbf{L}$ to every cell of $\mathbf{L}$, and f:$\mathbf{Q} \times \mathbf{Q}^k \to \mathbf{Q}$ is a function of the cell state transitions.

Every cell x has neighborhood $u(x) = (y_1, \ldots, y_k)$ such that $\forall y \in u(x)$: $|x - y|_{L_\infty} = 1$. The size of a neighborhood is $k = 8$ cells in a two-dimensional lattice and $k = 26$ cells in a three-dimensional lattice. The cell x being at state x^t at time step t calculates its next state x^{t+1} in accordance with the local transition function $x^{t+1} = f(x^t, u(x)^t)$. The transitions $+ \to -$ and $- \to .$ are unconditional. Therefore we have to define the only condition for transition $. \to +$, i.e., the condition of the excitation. The rule has the following form:

$$x^{t+1} = \begin{cases} + & x^t = . \quad \text{and} \quad \left|\{y \in u(x) : y^t = +\}\right| = \theta \\ - & x^t = + \\ . & \text{otherwise} \end{cases} \tag{1}$$

where $\theta = 2$ (lin two dimensions) and $\theta = 4$ (in three dimensions). The values of θ determine the name of the model version: the 2^+-medium and the 4^+-medium [4–6].

Proposition 1. The model $\mathbf{M}^+$ is simulated in the cellular automaton $\mathbf{A}$ with binary cell states and memory of capacity 1.

The automaton $\mathbf{A}$ has a partially determined cell state transition function $x^{t+1} = f(x^{t-1}, x^t, s(x)^t)$, where $s(x)^t = \Sigma_{y \in u(x)} y^t$; it is not determined on the set $(1, 1, a)$ of arguments for any a. For other arguments we have $f(0, 1, a) = 0$ and $f(1, 0, a) = 0$, for any a; $f(0, 0, \theta) = 1$ and $f(0, 0, a) = 0$ for $a \neq \theta$. So, the states of the cells of $\mathbf{M}^+$ are represented by the tuples of two first arguments: the rest state corresponds to 00, the excited states is represented by 01, and the refractory state is represented by 10.

4. MINIMAL PARTICLE-LIKE WAVES

Let $\mathbf{L}$ be the infinite lattice and $\sigma^t = \{x \in \mathbf{L} | x^t \in \{+, -\}\}$, $i \in \mathbf{N}$, be the finite subset of cells being in $+$ and $-$ states such that $\forall x \in \sigma^t \exists y \in \sigma^t : x \neq y$ and $x \in u(y)$ and $y \in u(x)$. Then σ^t is called a particle-like wave if it is translated by the parallel application of the function f to the cell neighborhoods.

Let $\mathbf{E} = \{0, \ldots, k\}$ be the set of all possible sums of excited elements of $u(x)$. The function f: $\mathbf{Q} \times \mathbf{Q}^k \to \mathbf{Q}$ belongs to the family Ξ of the multiple threshold excitations if it is determined by the rule

$$x^{t+1} = \begin{cases} + & x^t = . \quad \text{and} \quad \left|\{y \in u(x) : y^t = +\}\right| \in \Theta \\ - & x^t = + \\ . & \text{otherwise} \end{cases} \tag{2}$$

where $\Theta \in 2^{\mathbf{E}}$. The definition implies that the rest cell is excited if the sum of its excited neighbors matches one of the elements of Θ. The family Ξ includes all other possible functions of the lattice excitation with unconditional states transitions $- \to .$ and $+ \to -$.

Example 1. Let f be the function of the interval excitation defined by the rule

$$x^{t+1} = \begin{cases} + & x^t = . \quad \text{and} \quad \Gamma_1 \le \left|\{y \in u(x) : y^t = +\}\right| \le \Gamma_2 \\ - & x^t = + \\ . & \text{otherwise} \end{cases} \tag{3}$$

where $\Gamma_1 \le \Gamma_2$ and $\Gamma_1, \Gamma_2 \in \mathbf{E}$. To prove $f \in \Xi$ we show that $\Theta = \{a \in \mathbf{E} | \Gamma_1 \le a \le \Gamma_2\}$. Assuming that $\Gamma_2 = \max \mathbf{E}$, we demonstrate that all functions of conventional threshold excitations are elements of Ξ [7].

The configuration of the cellular automaton is the mapping c: $\mathbf{L} \to \mathbf{Q}$. Given the sequence $c^0 \to \ldots \to c^p$ of the configurations of $\mathbf{M}^+$, we say the function $f \in \Xi$, determined by Θ, is minimal in the family Ξ if for any other $f' \in \Xi$ determined by Θ', we have (i) $\left|\Theta\right| \le \left|\Theta'\right|$ and (ii) $\min \Theta \le \min \Theta'$.

In words, f is minimal if its corresponding set Θ has a minimal number of elements and the minimal element among the elements of all other characteristic sets of the elements of Ξ. In terms of the interval excitations this means that the cells have the only the interval of excitation, which is a singleton and the least possible element of $\mathbf{E}$.

Theorem 1. The rule (1) is the minimal rule of the excitation of two- and three-dimensional excitable lattices with near neighbor interactions that supports particle-like waves.

Proof. Let us consider the configurations of the particle-like waves. In a two-dimensional lattice the minimal translating pattern, the so-called 2^+-particle [4, 5, 6], consists of two excited and two refractory states. It moves along the coordinate axes. The configuration of the excited and refractory states encodes the orientation of the velocity vector as follows: north ($\begin{smallmatrix} + & + \\ - & - \end{smallmatrix}$), south ($\begin{smallmatrix} - & - \\ + & + \end{smallmatrix}$), west ($\begin{smallmatrix} + & - \\ + & - \end{smallmatrix}$), east ($\begin{smallmatrix} - & + \\ - & + \end{smallmatrix}$). To demonstrate nonstop movement we consider how many excited neighbors are around the rest cells surrounding the particle. Let us look at the 2^+ particle moving north:

$$\begin{array}{cccc} 1 & 2 & 2 & 1 \\ 1 & + & + & 1 \\ 1 & - & - & 1 \\ 0 & 0 & 0 & 0 \end{array}$$

In this scheme the states of excited and refractory cells are shown explicitly, whereas every rest cell contains the number of excited neighbors. We see that only two northern rest neighbors of the excited cells have two excited neighbors and, therefore, they are excited at the next step of discrete time; the currently excited cells become refractory and the pattern is shifted north.

In three-dimensional lattices the minimal particle-like waves, the so-called 4^+-particles, consist of 4 excited cell states and 4 refractory cell states. Every 4^+-particle can be imagined as the duplex of 2^+-particles (moving in parallel planes). The velocity vector of the 4^+-particle is parallel to one of the coordinate axes, perpendicular to the plane in which the block of $+$ states lies, and the orientation of the vector is encoded in the configuration of the $+$ and $-$ cells. Thus, e.g., the 4^+-particle, the velocity vector of which is collinear with y-axis, has the configuration

$$\begin{pmatrix} + & + \\ - & - \end{pmatrix}^{(x,y,x)} \quad \begin{pmatrix} + & + \\ - & - \end{pmatrix}^{(x,y,z+1)}$$

The rule (1) satisfies the condition (i) because Θ is a singleton. So, we need to prove condition (ii). In two-dimensional lattices $\theta = 2$, therefore, the only candidate to test is $\theta = 1$. Let the rest cell be excited if exactly one neighbor is excited. On infinite $\mathbf{L}$ any finite connected set σ^0, $|\sigma^0| \geq \theta$, of excited cells causes unbounded growth of excitation because the rest cells nearest to the extreme elements of the set have exactly one excited neighbor. Considering $\theta = 1, 2, 3$ in three-dimensional case, we obtain similar results. ■

More detailed considerations on the structure of minimal wave generators can be found in ref. 7.

Remark 1. The rule (1) is minimal only among models with spatially invariant cell state transition rules because some asymmetric neighborhoods of less size can also give translating patterns [7].

The minimal particles (2^+ and 4^+-particles) move along the rows or columns of the cell array.

Fortunately, there are also patterns that move along the diagonals of the arrays. They are 3^+-particles (in the two-dimensisonal lattice) and 6^+-particles (in the three-dimensional lattice). They consist of 3 $+$-states and 3 $-$-states, and 6 $+$-states and 6 $-$-states, respectively. Any 3^+-particle has 4 configurations (particle states) that are changed step by step in the loop. The diagonal movement is approximated by a series of ladder shifts (Fig. 3).

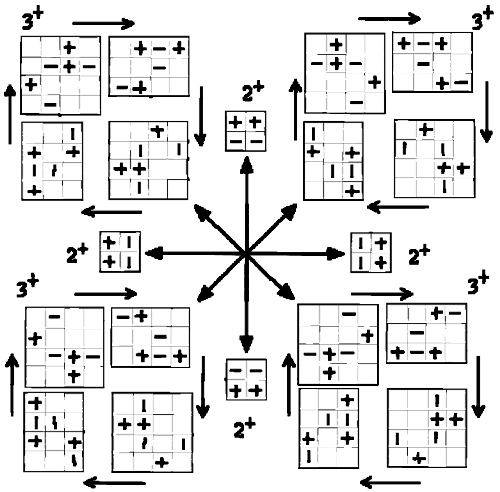

Fig. 3. Encoding of the directions of movement in the states of the minimal particles: two-dimensional lattice—2^+–medium.

The 6^+-particle can be imagined as the duplex of the 3^+-particles. The 6^+-particle moves in the plane parallel to one of the coordinate planes and only 2 of its 3 coordinates are changed during the movement.

Proposition 2. The 2^+-, 3^+-, 4^+-, and 6^+-particles are minimal indivisible compact movable patterns.

Proof. The mobility has been already proved when we considered the number of excited neighbors of the rest cells around the currently excited states. If, in the evolution of the model, we remove one of the excited states from any of the particles, the pattern disappears or is transformed into another pattern (rather not minimal). This was demonstrated by straightforward perturbations of the patterns [4]. The neighborhoods of the nonrest cells in the particles overlap; therefore these patterns are compact. The 2^+- and 4^+-particles are minimal because the number of excited cells in these patterns is equal to θ as defined in (1). Any compact pattern of excitation that includes less than θ excited cells will be entirely rest after few steps of the evolution. Using exhaustive search we prove that the 3^+- and 6^+-particles are the minimal patterns that move along the diagonals of the lattice. An example of a 4^+-particle is shown in Fig. 4. ■

Proposition 3. The velocity of 3^+- and 6^+-particles is four times less than the velocity of 2^+- and 4^+-particles.

More generally we can say that the patterns moving along the columns or rows of the lattice have unit velocity, whereas the velocity of the patterns

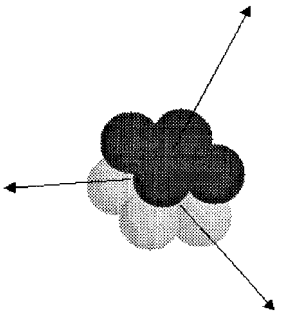

Fig. 4. 4^+–particle. Black spheres represent excited cells, light gray spheres are the refractory cells; rest cells are not shown.

running along diagonals is equal to 1/4 because the diagonal movement is approximated by ladder shifts along columns and rows [4].

Proposition 4. The minimal quantum of information in excitable lattices occupies a 2×2-cell volume in two-dimensional lattices and a $2 \times 2 \times 2$-cell volume in three-dimensional lattices.

5. PARTICLE GUNS: GENERATORS OF PARTICLE-LIKE WAVES

The constant 1 is realized by streams of particle-like waves. The streams are semiinfinite and they are produced by so-called particle guns. A particle gun is a finite compact pattern that periodically generates one or more types of particles. There is still no rigorous technique for the design of particle guns (however, identification algorithms [3] and integer programming [20] may be quite useful) and we base most of our propositions on the results of exhaustive search in a numerical experiments.

Proposition 5. There are no unmovable guns in 2^+-medium.

This is because there are no unmovable patterns in 2^+-medium at all (see Proposition 17).

Proposition 6. The minimal particle gun in 2^+-medium, the so-called G_2-gun, moves along one of the coordinate axes with unit velocity and has size of 6×9 cells and a weight of 26 nonrest states. The gun generates the 2^+-particle every fourth step of the evolution. The generated particles move in the direction opposite to the direction of the gun motion.

The configuration of a cellular automaton with a G_2-gun moving west and emitting 2^+-particles to the east is shown in Fig 5. The weight of the gun is maximal just before it delivers a new particle. Because the period of

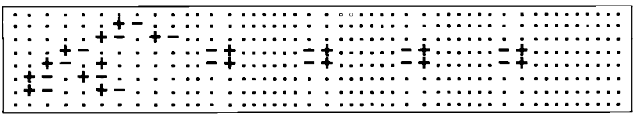

Fig. 5. Two-dimensional movable gun G_2.

generation is 4 time steps, the 2^+-particles are at distance 8 cells from each other. This determines the maximal frequency of the excitable computer.

In certain cases it may be extremely useful to have a gun that generates particles in the direction perpendicular to the velocity vector of the gun. Two minimal guns that generate particles in that manner are presented in Fig. 6 and 7. The first gun the G_3-gun, gives birth to $(2 + 1)^+$-particles (Fig. 6). As we will see later, the $(2 + 1)^+$-particle is transformed into the 2^+-particle via collision with another 2^+-particle. The G_3-gun has 18-nonrest state weight, 5×11-cell maximal size, and generate particles every fourth step of the evolution. The generated particles are grouped into the particle front. The distance between two particles in the front is 8 cells along the axes parallel to the velocity vector and 4 cells along the other axis.

The third gun, the G_2^7-gun, generates simulateously 2^+-particles and more complex patterns (of 7 excited states) every eighth step of the evolution (Fig. 7). The velocity vectors of all generated patterns are perpendicular to the velocity vectors of the gun. The 2^+-particles and 7^+-patterns move in opposite directions.

When talking about a minimal gun we should emphasize that the G_3-gun actually has less size and weight then the G_2-gun, though it does not produce elementary particles directly, but generates pro-particles that need additional collisions to be transformed into elementary particles. So we cannot accept the G_3-gun as minimal.

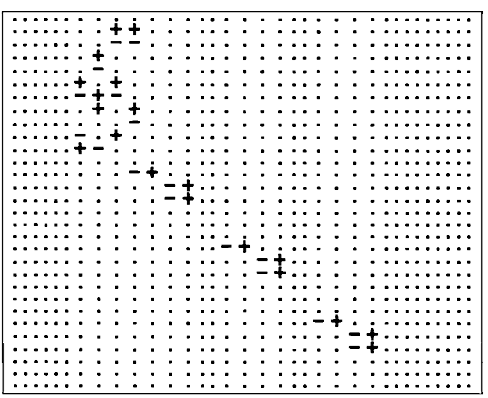

Fig. 6. Two-dimensional movable gun G_3.

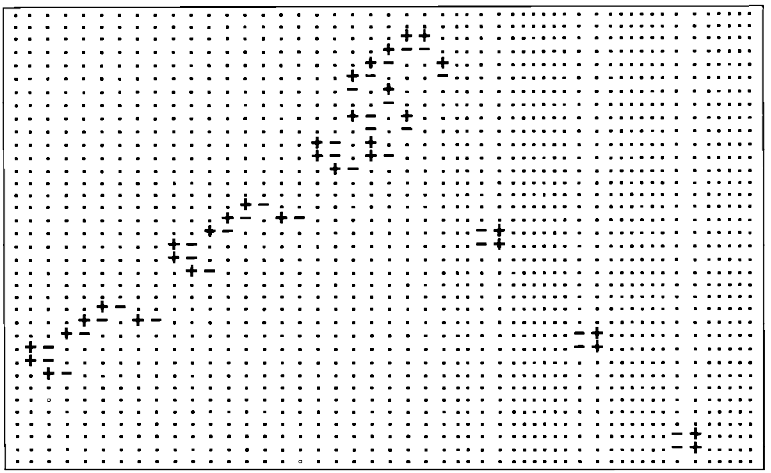

Fig. 7. Two-dimensional movable gun G_2^7.

Problem 1. Is it possible to generate a particle gun in a natural way, that is, in the collision of several elementary, 2^+- and 3^+-, particles?

There is no certain answer for two-dimensional lattices. In a three-dimensional lattice a stationary gun is generated via collision of two elementary particle-like waves.

Proposition 7. In the 4^+-medium the minimal mobile gun has a weight of 16 nonrest states, $4 \times 4 \times 3$ cell volume, and generates 4^+-particles every second step of the evolution. The generated 4^+-particles move in the direction opposite to the velocity vector of the gun.

The gun is shown in Fig. 8. It moves along one of the coordinate axes. It is very elegant and can be built from a 4^+-particle by adding 4 additional excited states and placing them at the angles of the quadruple of the refractory states (Fig. 8, *t*). The new 4^+-particles are launched at the back of the gun and move in directions opposite to the gun velocity vector. The gun forms an extremely dense stream of 4^+-particles with only 2 empty cell distance between the neighboring particles.

Proposition 8. In the 4^+-medium the minimal stationary gun, the G_2^4-gun, has 12 nonrest state weight, $4 \times 4 \times 3$ cell volume, and generates two 4^+-particles every third step of the evolution.

The development of the G_2^7-gun is shown in Fig. 9. When generating the particles the gun changes its state in a cycle of length 3. It subsequently takes the following proper states: (i) an empty square with excited boundaries, or 8 excited states (Fig. 9, *t*), (ii) a plate of 4 excited states surrounded by

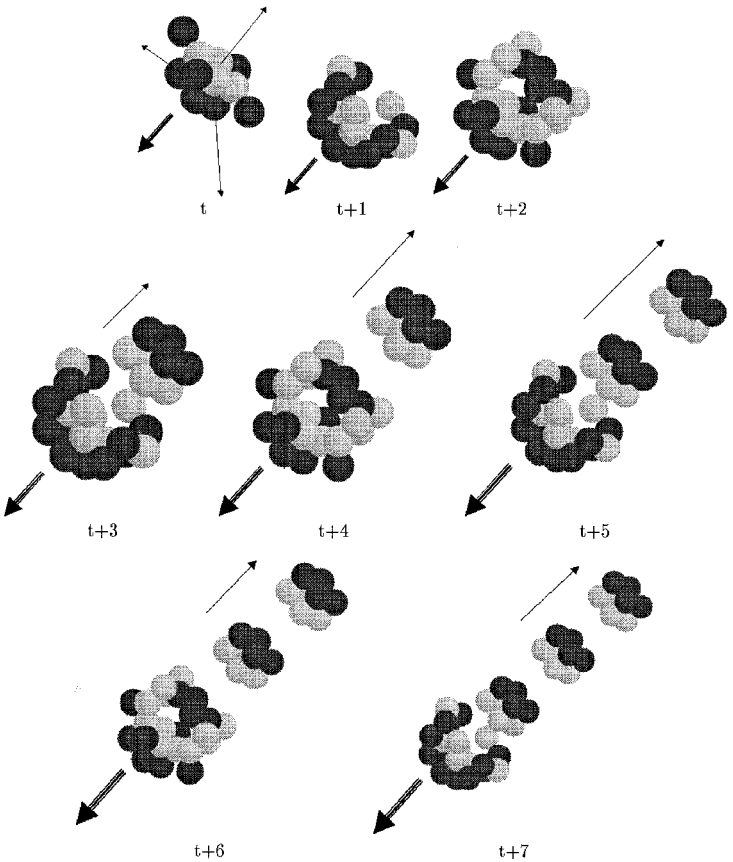

Fig. 8. Mobile gun in 4^+–medium (three-dimensional excitable lattice). Coordinate axes are indicated on the first image. The double arrow shows the direction of gun motion. Black spheres represent excited cells, light gray spheres are the refractory cells; rest cells are not shown.

8 refractory states (Figure 9, $t + 1$), and (iii) a plate of 4 refractory states sandwiched between the plates of 4 excited states (Figure 9, $t + 2$).

Proposition 9. A three-dimensional stationary gun, the G_2^4-gun, is generated as a result of frontal collision of two 6^+-particles.

The scheme and the skeleton of the collision are shown in Fig. 10. Parameters of the collision are described in the Appendix. It is remarkable that slight relative shifts of the colliding 6^+-particles change the orientation of the G_2^4-gun by 90°.

Proposition 10. All guns are destroyable.

This is trivially proved by the collision of 2^+- and 4^+-particles with particle guns. Collision is followed by short-range perturbation (dissipation

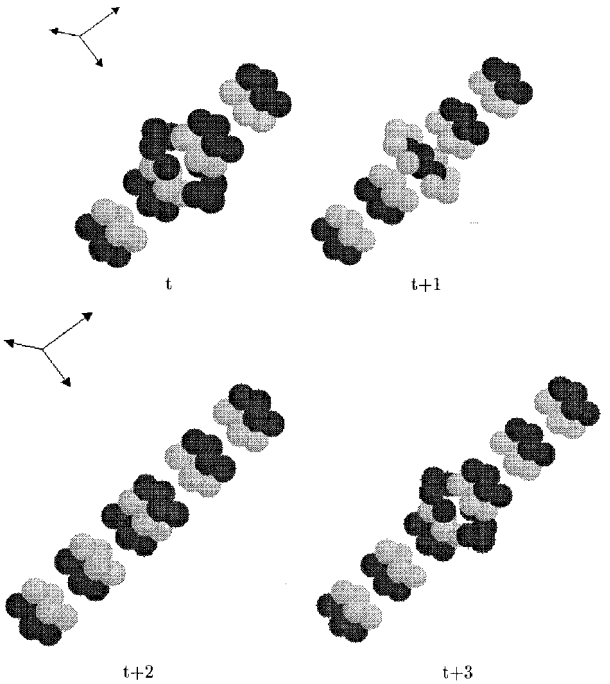

Fig. 9. Stationary three-dimensional gun G_2^4.

of energy), after which all patterns of excitation disappear. The following important problem remains open.

Problem 2. Are there generators of 3^+- and 6^+-particles in the excitable lattices?

6. COLLISIONS AND INTERACTION GATES

Self-localized excitations, or particle like waves, represent the bits of information (or unit impulses) and logical gates are realized when two or more particles collide one with another. The logical operations are implemented at the sites of collision when two or more particle-like waves interact with one another. Therefore logical gates realized in excitable media are called interaction gates. In general, the result of a collision is determined by the types and phases of colliding particles and the angle of collision. To build the structure of all interaction logical gates in excitable lattices we collided the particles in all combinations in an entirely rest environment. Surprisingly, we found that excitable lattices support a much wider range of interaction gates than any oher automata model.

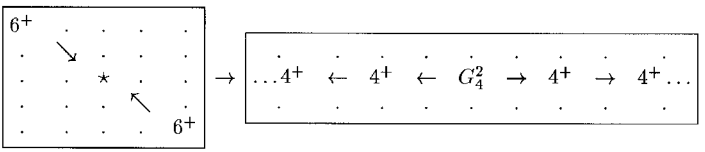

A.

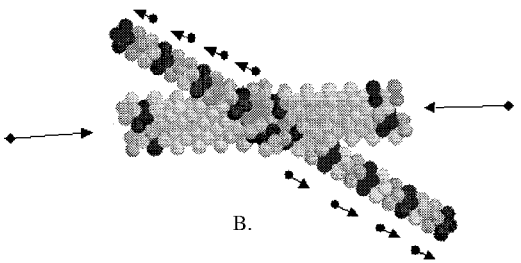

B.

Fig. 10. The scheme (A) and the skeleton (B) of the frontal collision of two 6^+–particles that leads to formation of the stationary G_2^4-gun, which generates 4^+–particles.

A typical interaction gate has two input wires (by *wire* we mean trajectory of the particle-like wave) and at least two, but usually three, output wires. Two output wires represent the trajectories of particles when they continue their motion undisturbed and the third output wire represents the trajectory of a new particle formed as the result of collision of two incoming particles.

To describe the interaction gates we use two symbols: $\triangle$ and $\triangledown$. The $\triangle$ symbol indicates that the results of the collision appear in parallel on different output wires/trajectories. The $\triangledown$ shows that the resulting particles appear exclusively on one of the outputs. Thus, e.g., the billiard ball gate (Fig. 1) is represented as

$$\langle x, y\rangle \to x\bar{y} \triangledown \bar{x}y \triangledown (xy \triangle xy).$$

The glider interaction gate (2) of the game of Life is described in the following form:

$$\langle x, y\rangle \to x\bar{y} \triangledown \bar{x}y.$$

When specifying the product of the interaction gates we also indicate (in brackets) which particle-like waves present the terms of the gates. The specification is monotonous in the case of the billiard ball gate

$$\langle \text{ball, ball}\rangle \to \text{ball} \triangledown \text{ball} \triangledown (\text{ball} \triangle \text{ball})$$

and the glider gate

$$\langle \text{glider, glider} \rangle \to \text{glider} \bigtriangledown \text{glider}.$$

but becomes very interesting when excitable media are considered. The next result deals with a two-dimensional excitable lattice.

Proposition 11. The following types of interaction gates are realized in a 2^+-medium:

$g1(x, y) = \bar{x}y \bigtriangledown x\bar{y}$ $[\langle 2^+, 2^+ \rangle \to 2^+ \bigtriangledown 2^+]$
$g2(x, y) = (xy \bigtriangleup xy) \bigtriangledown \bar{x}y \bigtriangledown y\bar{x}$ $[\langle 2^+, 2^+ \rangle \to (2^+ \bigtriangleup 2^+) \bigtriangledown 2^+ \bigtriangledown 2^+]$
$g3(x, y) = xy \bigtriangledown \bar{x}y \bigtriangledown x\bar{y}$ $[\langle 2^+, 2^+ \rangle \to 3^+ \bigtriangledown 2^+ \bigtriangledown 2^+]$
$g4(x, y) = g3(x, y)$ $[\langle 2^+, 3^+ \rangle \to 3^+ \bigtriangledown 2^+ \bigtriangledown 3^+]$
$g5(x, y) = xy \bigtriangledown \bar{x}y \bigtriangledown x\bar{y}$ $[\langle 2^+, 2^+ \rangle \to (2 + 1)^+ \bigtriangledown 2^+ \bigtriangledown 2^+]$
$g5a(x, y) = xy \bigtriangleup xy$ $[\langle (2 + 1)^+, 2^+ \rangle \to 2^+ \bigtriangleup 3^+]$
$g6(x, y) = xy \bigtriangledown \bar{x}y \bigtriangledown x\bar{y}$ $[\langle 3^+, 2^+ \rangle \to 2^+ \bigtriangledown 2^+ \bigtriangledown 3^+]$
$g7(x, y) = y \bigtriangleup [\bar{x}y \bigtriangledown xy]$ $[\langle 3^+, 2^+ \rangle \to 2^+ \bigtriangleup (3^+ \bigtriangledown 2^+)]$

Proof. A catalog of gates is shown in Fig. 11. The absolute orientation of the wires reflects the orientation of velocity vectors of the particles

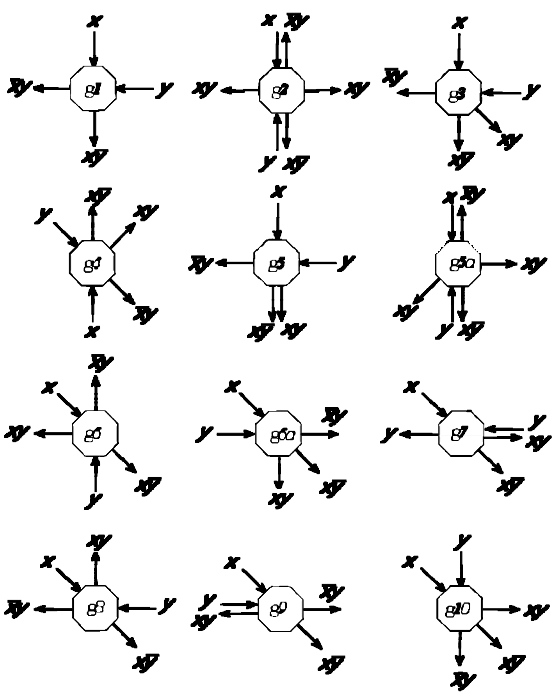

Fig. 11. The interaction gates realizable in a two-dimensional excitable lattice—2^+–medium.

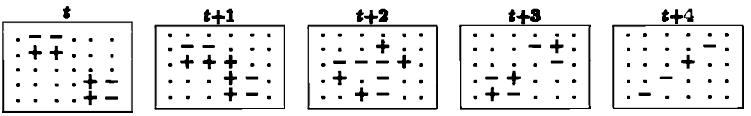

Fig. 12. Gate $g1$.

approaching the collision site and leaving the collision site. The vertical and horizontal arrows represent trajectories of 2^+-particles [or 2^+-like particles as, e.g., a $(2 + 1)^+$-pattern], and diagonal arrows are the trajectories of the 3^+-particles. When we show the evolution of the excitable lattice that realizes one of the gates we assume $x = 1$ and $y = 1$, i.e., two particles approach the collision site simultaneously.

The first gate, $g1$ is a typical glider gate (as in the game of Life). When two 2^+-particles collide (Fig. 12, t) they destroy each other (Fig. 12, $t + 4$) and disappear. The $\bar{x}y$ is computed as the result of such a collision.

Colliding 2^+-particles frontally (Fig. 13, t) we realize xy in gate $g2$. The 2^+-particles collide quasielastically and change directions of their motion as the result of collision. The first two gates involve only 2^+-particles. All other gates use also 3^+-particle as the outcome of the collision.

In the $g3$ gate a 3^+-particle is formed when two 2^+-particles come into a front-by-side collision as specified in Fig. 14. The 3^+-particle represents the xy product of the logical operation. When a 2^+-particle moving west crashes into a 2^+-particle moving south (Fig. 14, t) a 3^+-particle is formed and it moves southeast (Fig. 14, $t + 5$).

The $g4$ gate is a very typical example of an excitable interaction gate (Fig. 15). The x variable is represented by a 3^+-particle moving southeast when $x = 1$ and the y variable is represented by a 2^+-particle moving north when $y = 1$. When the particles collide ($t + 1$) a new self-localized excitation—3^+-particle—is formed ($t + 6$). This particle moves northeast. If $y = 0$ and $x = 1$, then the 2^+-particle simply continues its motion and we have 1 on the $x\bar{y}$ output trajectory. If $x = 0$ and $y = 1$, we register a 3^+-particle on the $\bar{x}y$ output trajectory.

The $g5$ gate is one of the most attractive. At first sight it is similar to the $g1$ gate because we obtain $\bar{x}y$ and $x\bar{y}$ results from the same wires as in the $g1$ gate (Fig. 11). It also computes the xy function. However, if $x = 1$ and $y = 1$, the product xy is represented by a $(2 + 1)^+$-pattern (Fig. 16).

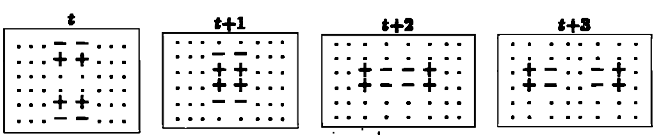

Fig. 13. Gate $g2$.

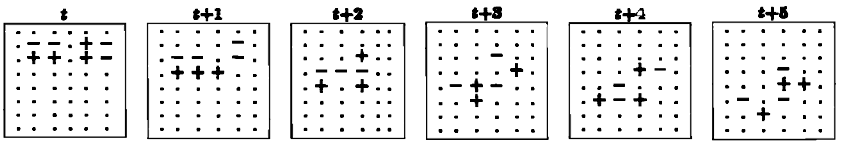

Fig. 14. Gate $g3$.

This is the only gate where we allow representation of a variable value by a nonelementary particle-wave. It is because the 2^+- and $(2 + 1)^+$-patterns can be easily differentiated in the collision with another 2^+-particle (Fig. 17). Let p be an unknown pattern [either 2^+- or $(2 + 1)^+$-pattern] that represents the result of a computation in the $g5(1, y)$ gate. Then we compute $g5a(p, 1)$. If p is represented by a $(2 + 1)^+$-pattern, then the southwest 'wire' of the $g5a$ gate gives a 3^+-particle. If p is represented by a 2^+-particle (i.e., $x\bar{y}$ result of a $g5$ gate), then we have nothing on the southwest wire of the $g5a$ gate.

The next two gates, $g6$ and $g6a$, are equivalent in almost all respects (Figs. 18 and 19) except the orientations of the input wires: the x and y variables are represented by 3^+- and 2^+-particles, the $x\bar{y}$ term is represented by a 3^+-particle, and the $\bar{x}y$ and xy terms by 2^+-particles, respectively.

Gate $g7$ gives an example of the deflection of one particle by another particle where the second one does not change its trajectory (Fig. 20). When $x = 1$ and $y = 1$ in the $g7$ gate a 3^+-particle moving southeast comes into collision with 2^+-particle moving west. As the result of the collision the 2^+-particle continues its journey undisturbed, but the 3^+-particle is transformed into a 2^+-particle that runs east. ■

The three remaining gates (Fig. 11), $g8$, $g9$, and $g10$, are actually equivalent to one of the previous gates except for the relative orientation of the trajectories of incoming particles.

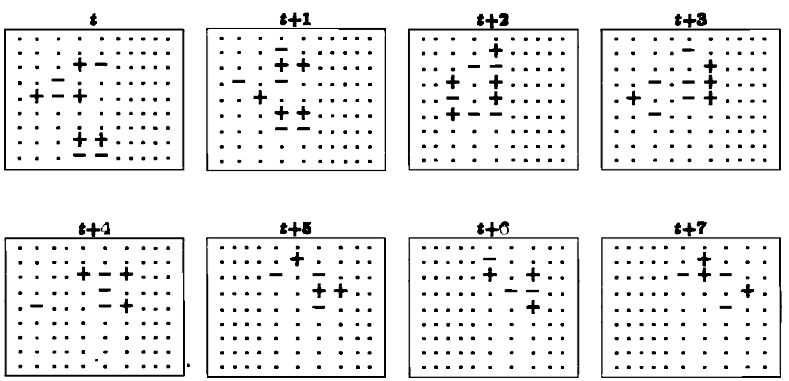

Fig. 15. Gate $g4$.

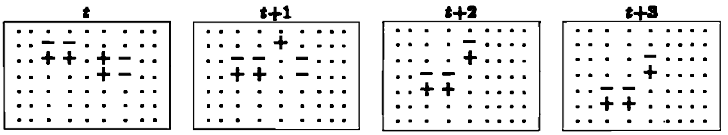

Fig. 16. Gate $g5$.

Proposition 12. All gates except $g2$, $g5a$, $g7$, and $g9$ do not alter data.

The data are assumed to be altered by the result of the computation when at least one of the outcoming particles goes along the same trajectory as one of the incoming particles. The data are altered in two different ways. The $g2$ and $g5a$ gates alter data weakly (Fig. 11) because the particle representing $\bar{x}y$ goes on the trajectory of x only when $x = 1$. The $g7$ and $g9$ gates alter data sufficiently because the particle representing xy goes along the trajectory of the particle representing y when $x = 1$ and $y = 1$ (Fig. 11).

Proposition 13. The $g2$ gate is excitation conservative.

The gate is excitation conservative because (i) the number of the incoming particles is equal to the number of outcoming particles, and (ii) the numbers of overall excited states before and after collision (before and after computation) are equal to each other (Fig. 13).

Proposition 14. The minimal $x \wedge y$ and $\bar{x} \wedge y$ gates in the 2^+-medium have 2 input and 3 output wires and (5×2) cell size.

Let $\gamma(g)$ be the size of a gate g, i.e., the maximum among the sizes of the input and output particles, and sizes of the collision and perturbation areas. Then we have following space complexities of the gates: $\gamma(g1) = (5 \times 5)$, $\gamma(g2) = (4 \times 2)$, $\gamma(g3) = (5 \times 2)$, $\gamma(g4) = (4 \times 6)$, $\gamma(g5) = (5 \times 3)$, $\gamma(g5a) = (3 \times 6)$, $\gamma(g6) = (4 \times 7)$, $\gamma(g6a) = (7 \times 4)$, $\gamma(g8) = (5 \times 6)$, $\gamma(g9) = (7 \times 3)$, and $\gamma(g10) = (4 \times 7)$. The $g2$ gate has minimal size. Unfortunately, it does alter inputs (Fig. 11). The $g3$ is slightly larger than $g2$, but does not alter data. It covers a 10-cell area and computes both $x \wedge y$ and $\bar{x} \wedge y$ functions.

Reusability of the computing device is one of the advantages of excitable lattice computations. To start a new computational process on the same lattice we clean up all results of the previous computations. If the lattice has absorbed boundaries, this is not a problem. As it was proved in ref. 7 for 2^+-medium, the evolution started at any random configuration of the excited and refractory

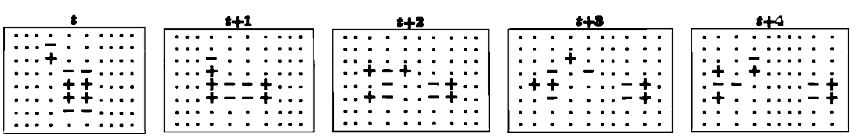

Fig. 17. Gate $g5a$.

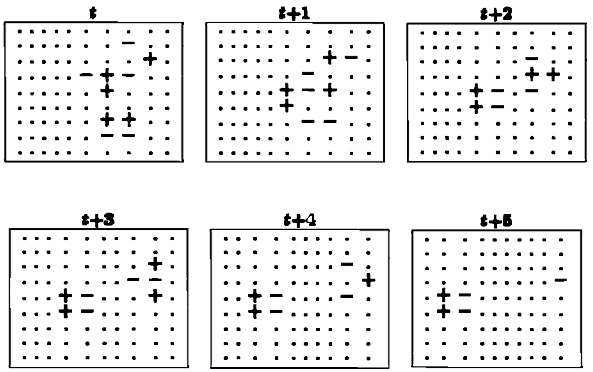

Fig. 18. Gate g_6.

states of the lattice nodes is completed in the entirely-rest lattice. In the case of periodic boundaries there is a possibility that several particle-like waves will travel on this discrete torus along nonintersecting trajectories. Here we can use the so-called erase collision (Fig. 21) to clean up the lattice. To form the *cleaner* we collide a 2^+-particle with a 3^+-particle (Fig. 21, t, . . . , t + 3). As the result of collision a movable growing pattern is formed (Fig. 21, t + 10, . . . , t + 16). The pattern has two growth points. They move

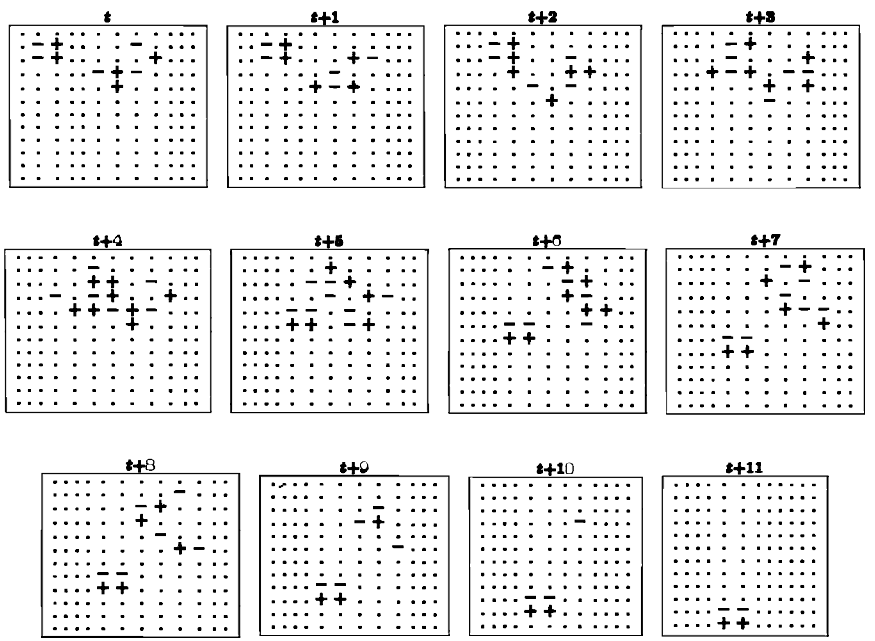

Fig. 19. Gate *g6a*.

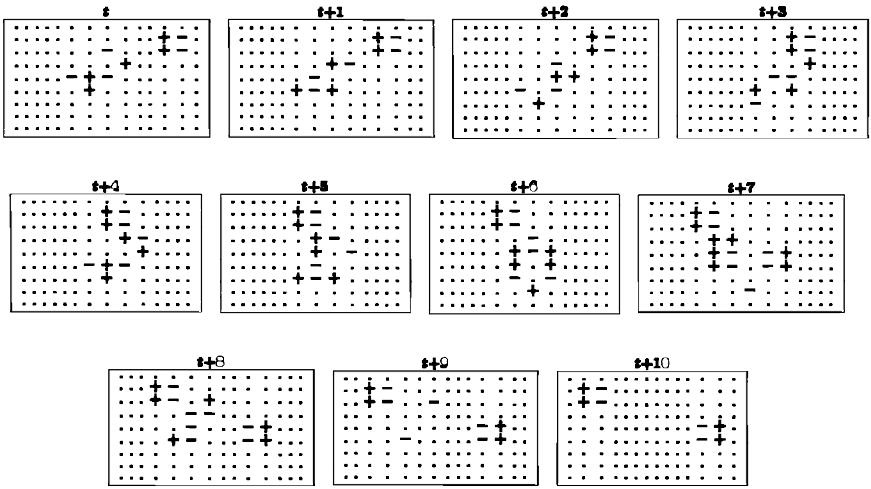

Fig. 20. Gate $g7$.

perpendicular to each other. Therefore the pattern is stretched (Fig. 22). If any particle collides into the pattern body the particle disappears. To kill the cleaner we crash 2^+-particles into the growth points of the cleaner.

Proposition 15. The following types of interaction gates are realized in 4^+-medium:

$h1(x, y) = x\bar{y} \vee \bar{x}y$ $[\langle 4^+, 4^+\rangle \to 4^+ \vee 4^+]$ or $[\langle 6^+, 6^+\rangle \to 6^+ \vee 6^+]$ or $[\langle 4^+, 6^+\rangle \to 4^+ \vee 6^+]$
$h2(x, y) = xy \vee x\bar{y} \vee \bar{x}y$ $[\langle 4^+, 6^+\rangle \to 4^+ \vee 4^+ \vee 4^+]$
$h3(x, y) = x\bar{y} \vee y$ $[\langle 4^+, 6^+\rangle \to 4^+ \vee 6^+]$
$h4(x, y) = (xy \wedge xy) \vee x\bar{y} \vee \bar{x}y$ $[\langle 4^+, 6^+\rangle \to (4^+ \wedge 4^+) \vee 4^+ \vee 6^+]$
$h5(x, y) = 1$ $[\langle 6^+, 6^+ \to G_4^2]$
$h6(x, y, z) = (xyz \wedge xyz \wedge xyz \wedge xyz \wedge) \vee \bar{x}yz \vee \bar{x}y\bar{z} \vee x\bar{y}z$
$[\langle 6^+, 6^+, 6^+\rangle \to (4^+ \wedge 4^+ \wedge 4^+ \wedge 4^+) \vee 6^+ \vee 6^+ \vee 6^+ \vee 6^+]$

The $h1$ and h2 gates are similar to the $g1$ and $g10$ gates of the 2^+-medium. The coordinates of excited and refractory cells before the collision in the $h2$-gate are presented in the Appendix; an example of the collision is shown in Fig. 23.

In the collision between 4^+- and 6^+-particles in the $h3$ gate a new 6^+-particle is generated. It moves along the same trajectory as the previous 6^+-particle when approaching the collision site (Fig. 24).

When two particles interact with each other in the $h4$ gate they give birth to two 4^+-particles. These new 4^+-particles move perpendicularly to the plane of collision. The skeleton of the collision is shown in Fig. 25; the

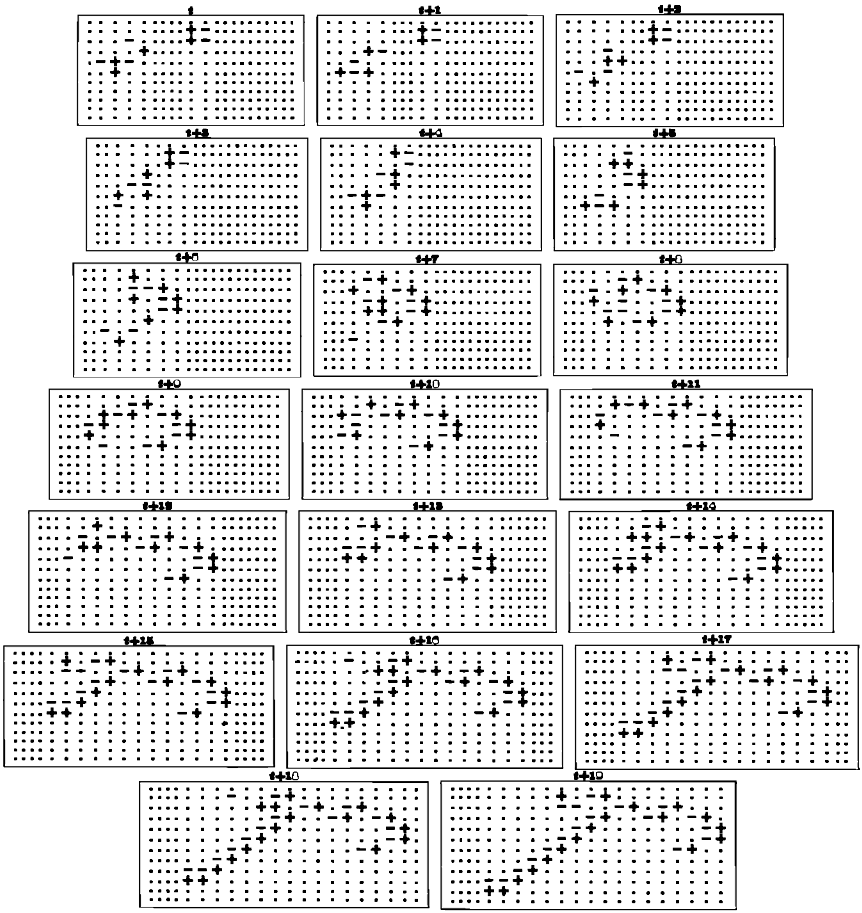

Fig. 21. Erase collision.

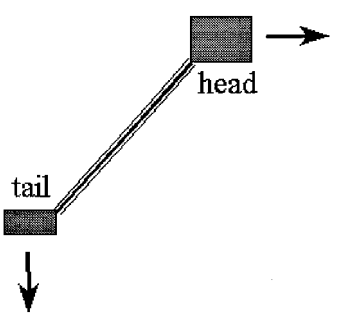

Fig. 22. Architecture of cleaner.

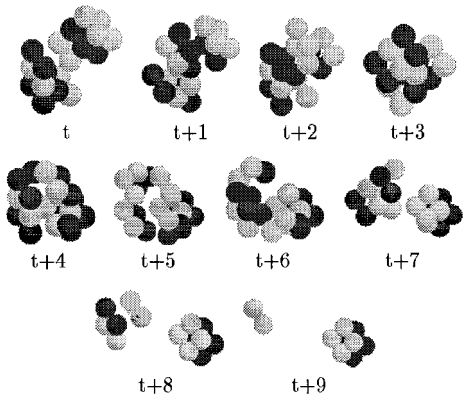

Fig. 23. $h2$–gate: collision of a 4^+–particle with a 6^+–particle; the 4^+–particle is formed as the result of collision.

coordinates of excited and refractory cells representing positions of 6^+- and 4^+-particles before collision are shown in the Appendix. The $h5$ collision is discussed in Section 7 and the Appendix.

A quadruple of 4^+-particles is formed when the ternary collision of 6^+-particles takes place in the $h6$-gate. The scheme and the skeleton of the collision are shown in Fig. 26. The positions of colliding particles and complete history of the collision can be found in the Appendix.

7. REFLECTORS, COUNTERS, AND REGISTERS

In the Fredkin–Toffoli model [45, 58] stationary mirrors are used to deflect the trajectory of a signal, make a sideways shift, implement a delay, or realize a crossover of two signals. In the cellular-automata models the stationary mirrors are usually represented by stationary patterns of the nonrest

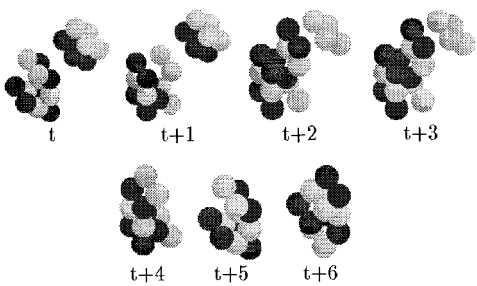

Fig. 24. $h3$ gate: collision of a 4^+–particle with a 6^+–particle with the formation of a 6^+–particle.

cell states [58]. In this section we also analyze unmovable self-localized patterns (that is, patterns that do not change their size globally, do not translate on the lattice, and do not generate other patterns) in excitable lattices and examine possible ways to realize deflections of particle-like waves and to construct counters and registers.

Proposition 16. If there is an unmovable pattern in an excitable lattice, then it is an oscillator.

The transitions $+ \to -$ and $- \to .$ are unconditional, therefore any configuration σ_1 of excited cells at time t transforms into a configuration of refractory cells at time $t + 1$ and comes to rest at $t + 2$. Before the excited cells of σ_1 become refractory they excite some of the surrounding cells of σ_2, which, in turn, excite the third pool σ_3 of cells. If the cells of σ_1 lie in the neighborhood of cells from σ_3 they will be excited at time $t + 3$.

Unfortunately, the following fact holds for two-dimensional lattices.

Proposition 17. There are no unmovable patterns in a 2^+-medium.

Let the pattern exist. Then it has at least two excited cells and at least two refractory cells. In any connected set of excited and refractory cells in a two-dimensional lattice there are couples of neighboring excited cells that have more than one rest neighbor. These rest neighbors will be excited and they also have more than one rest neighbor. So, the diameter of the excited set will grow. A more detailed treatment of the subject, investigating minimal generators, is presented in ref. 7. The outcome of the proposition states that there are no stationary reflectors nor stationary registers in two-dimensional excitable lattices.

Proposition 18. The minimal unmovable pattern in a 4^+-medium has 12 non-rest-state weight, $3 \times 3 \times 3$ cell volume, and oscillates with period 3.

The pattern, the so-called blinker B, has three configurations, which are changed in the loop $c_1 \to c_2 \to c_3 \to c_1$. In the $[(x, y, z), (x, y, z + 1), x, y, z + 2)]$-slices the states of B are changed in the following manner:

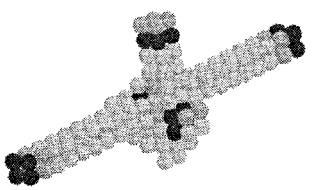

Fig. 25. Skeleton of the collision in the $h4$ gate.

$$c_1 = \left[\begin{pmatrix} \cdot & + & \cdot \\ - & + & - \\ \cdot & + & \cdot \end{pmatrix} \begin{pmatrix} \cdot & \cdot & \cdot \\ - & \cdot & - \\ \cdot & \cdot & \cdot \end{pmatrix} \begin{pmatrix} \cdot & + & \cdot \\ - & + & - \\ \cdot & + & \cdot \end{pmatrix} \right]$$

$$c_2 = \left[\begin{pmatrix} \cdot & - & \cdot \\ \cdot & - & \cdot \\ \cdot & - & \cdot \end{pmatrix} \begin{pmatrix} + & + & + \\ \cdot & \cdot & \cdot \\ + & + & + \end{pmatrix} \begin{pmatrix} \cdot & - & \cdot \\ \cdot & - & \cdot \\ \cdot & - & \cdot \end{pmatrix} \right]$$

$$c_3 = \left[\begin{pmatrix} \cdot & \cdot & \cdot \\ + & \cdot & + \\ \cdot & \cdot & \cdot \end{pmatrix} \begin{pmatrix} - & - & - \\ + & \cdot & + \\ - & - & - \end{pmatrix} \begin{pmatrix} \cdot & \cdot & \cdot \\ + & \cdot & + \\ \cdot & \cdot & \cdot \end{pmatrix} \right]$$

The period of 3 time steps is the minimal possible period of the oscillation. It follows from the cell state transition rule: a cell excited at time step

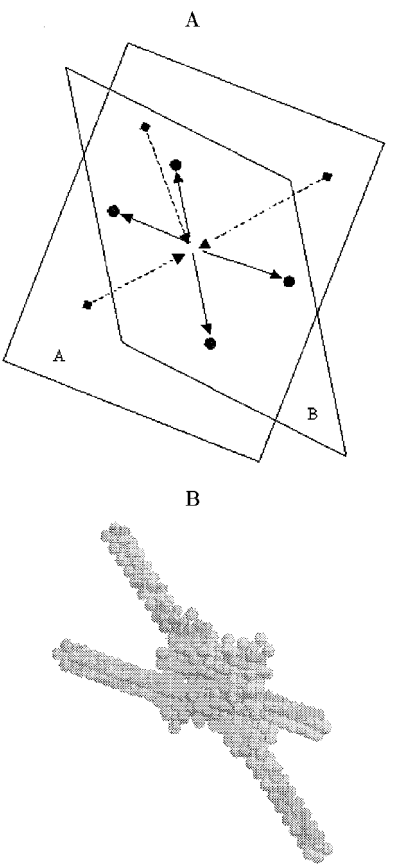

Fig. 26. Scheme (A) and the skeleton (B) of the collision of three 6^+–particles with the formation of four 4^+–particles in the $h6$–gate.

t can be excited again only at time step not less than $t + 3$ because it has a refractory state at step $t + 1$ and the cell returns to the rest state at step $t + 2$.

Proposition 19. As a result of collision with the B blinker a 4^+-particle is destroyed. The B may be destroyed or not destroyed depending on the phase differences of the patterns just before collision.

This finding is the result of an exhaustive search of all possible collisions between 4^+-particles and the B blinker. Arranging several copies of the blinker on a lattice and specifying the distances between them, we can realize registration. We still do not know if it is possible to generate the B blinker in the collision of 4^+- or 6^+-particles; therefore currently we are able to design the read only registers in the 4^+-medium. Another consequence of the previous propositions claims the following:

Proposition 20. There are no unmovable reflectors in excitable lattices.

As we found in Section 6, every elementary particle may play the role of a mobile reflector.

Proposition 21. In 2^+-medium the mobile counter representing m digits is a movable pattern of $2 + m$ excited states. It has the size of $2(m + 1) \times (2 + m)$ cells.

The counter representing 0 is a 2^+-particle. To increment the value of the counter we collide the 2^+-particle into the counter pattern, e.g.,

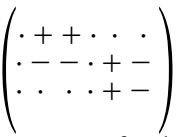

As the result of the collision a counter of value 1 is formed,

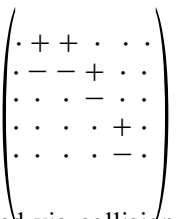

Every next increment is realized via collision of a 2^+-particle with the *tail* of the counter pattern in the following manner:

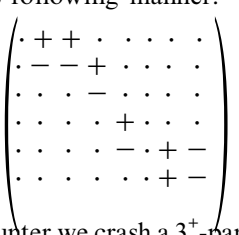

To decrement value of the counter we crash a 3^+-particle into the end of the *tail*.

8. EXCITABLE LATTICES AND GAMES OF LIFE: COMPARATIVE STUDY

What place do excitable lattices take in the hierarchy of models of universal computation? Here we compare our models with nonstandard computationally universal machines.

The first candidate, *Bank's computer* [12], has stationary architecture: predetermined wires and gates are represented in combination of the non-rest-cell states.

The *Life without Death* [48] model has no predetermined architecture and simulates interaction gates of the billiard ball model quite explicitly. However, all trajectories of the signals are represented in the non-rest-cell states, which are absorbing states in the cell evolution. That is, the full history of the computation in the *Life without Death* model can be extracted from the final stationary configuration. The model is not reusable, which is a very small, but still notable disadvantage.

The interpretation of the billiard ball model in a two-dimensional *partition cellular automaton* [58] seems to be slightly artificial. Actually, the 16 states which are used in the cellular-automata model are quite enough to encode the motion of an abstract object in 8 directions (on an integer lattice) and to adjust collisions and reflections in the conventional cellular-automata model.

The *sandpile* model [49] has at least three cell states and allows us to perform computation using one-dimensional gliders moving on linear graphs. A sandpile computer should have stationary quasi-one-dimensional architecture. It is impossible to build nontrivial particle-like patterns on the lattice in the two-dimensional sandpile model. The trivial patterns would be analogues of the ladder-like pattern that grows in lattice fire models (i.e. the refractory state is an absorbing state).

Therefore, the only candidate to compare with the ecitable lattice is the *game of Life* model [47, 15]. Both the excitable lattice and game of Life models exhibit bounded growth from a randomly chosen configuration and represent binary signals by translating patterns, called gliders and particle-like waves. The game of Life is obviously minimal in number of cell states. Both models have exactly the same cell neighborhoods. The game of Life is the unquestionable winner in terms of the complexity of unmovable patterns. But it loses in all other parameters. Excitable lattices have smaller and lighter self-localized movable patterns and stationary guns. The game of Life has no mobile guns at all. Excitable lattices have them. The only gate realizable in a single binary collision of gliders in the game of Life is $x \underline{\wedge} y$, whereas we can compute both $\bar{x} \underline{\wedge} y$ and $x \underline{\wedge} y$ in the single collision of two particle-like

waves in excitable lattices. The exact parameters of the elementary objects in these two models are shown in Table I.

Here we also notice that in three dimensions only the 4555, 5766, and 5655 rules exhibit gliders and bounded growth from random configuration [13]. Bays [13] accentuates that gliders should occur naturally in evolution, i.e., they hae to appear reasonably often. However, as he mentions, gliders in the 5655 rule are extremely rare and glider guns have not been discovered. In contrast, 4^+- and 6^+-particles are stable solutions in every numerical experiment with excitable lattices. Moreover, the particle guns emerge in every series of at most 100 experiments with a 4^+-medium.

Remarkably, there are no generators of spaceships, i.e., particles moving along coordinate axes, in the game of Life; in excitable media there are no generators of 3^+- and 6^+-particles.

9. REAL-LIFE CANDIDATES

Nonlinear media that exhibit self-localized mobile patterns in their evolution are potential candidates for the role of universal dynamical computers. Here we tackle a few of the models: breathers, solitons, light bullets, and a couple of exotic findings.

9.1. Solitons

The one-dimensional cellular automata models of solitons have been widely recognized since the papers by Park, Steiglitz, and Papatheodoru *et*

Table I. Elementary Parameters of the Game of Life and Excitable Lattices[a]

Parameter	2D game of Life	3D game of Life	2D excitable lattice	3D excitable lattice
Minimal stationary patterns	(4, 4)	(7, 8)	No	(12, 27)
Minimal mobile pattern (moving along columns or rows)	(8, 16)	(18, 40)	(4, 4)	(8, 8)
Minimal mobile pattern (moving along diagonals)	(5, 9)	No	(6, 16)	(16, 32)
Minimal stationary gun	(45, 180, 30)	No	No	(12, 48, 3)
Minimal mobile gun	No	No	(26, 54, 4)	(16, 48, 2)
One-collision logical gate	$x \wedge y$	$x \wedge y$	$x \wedge y$ and $x \vee y$	$x \wedge y$ and $x \vee y$

[a] Complexity of the particle-like waves and stationary patterns is written in the format (*weight, volume*), where *weight* is the number of the non-rest-cells. Complexity of the particle guns has the format (*weight, volume, period of particle generation*). Parameters of the three-dimensional game of Life model were evaluated for the 5655 rule [13].

al. [62, 74, 63]. Several classes of (ir)reversible cellular automata were characterized by soliton-like patterns [2, 46]. One particular class of soliton automata on chemical graphs was invented and carefully investigated by Dassow and Jurgensen [29, 30]. Recent results on soliton automata include transformation of the discrete soliton equations into binary cellular automata [77, 19] and construction of integrable cellular automaton with an N-soliton solution [78]. Unfortunately, solitons pass through each other in collisions (even on discrete lattices) (see, e.g., ref. 35), which significantly complicates the possible realizations of the interaction gates. In this case the only usable solution refers to particle machines and measures of information transfer in soliton collisions [52].

9.2. Light Bullets

Still being considered widely as three-dimensional solitons, light bullets never survive collision without loss of energy [17, 36]. Therefore they are quite suitable for interaction gates. The results of numerical simulations of three-dimensional generalized nonlinear Schrödinger equations in a model with alternative refractive index demonstrate the propagation of the stable light bullets with soliton-like behavior [36, 37].

There are several computationally useful outcomes of bullet binary collisions [38]: (1) light bullets survive collision, (2) two bullets fuse into a stationary wave, (3) bullets pass through each other, but a third stationary wave is formed, and (4) bullets rotate around one another and change their outcoming trajectories.

Finding 1. The $g2$ gate is realized in light bullet interactions. This follows from the results of the simulation of light bullets [38]. In the $g2$ gate the input trajectories of x and y variables are coincident with the output trajectories of $\bar{x}y$ and $x\bar{y}$ terms, respectively. The value of xy can be registered from two different outward trajectories (Fig. 13). An example of the $g2$ gate is given by spiraling light bullets [38]. When two light bullets move toward one another and collide side by side with a certain offset they rotate around one another without capture or fusion, and later escape the interaction zone with transverse velocities [38].

Let λ^+ be a moving light bullet and λ^0 be a stationary solution (nonmoving bullet). Then two following interaction gates are realized in the light bullet collision.

Finding 2. $h_1(x, y) = \bar{x}y \triangledown x\bar{y} \triangledown (xy \Delta xy \Delta xy)$ $[\langle \lambda^+, \lambda^+ \rangle \rightarrow \lambda^+ \triangledown \lambda^+ \triangledown (\lambda^+ \Delta \lambda^0 \Delta \lambda^+)]$. This is the situation of fission [38]: the bullets move toward each other, pass through each other, and continue their motion, but a third stationary wave is also formed. It stays at the site of collision. There are two

waves before the collision and three waves after it. The stationary wave represents *xy*.

Finding 3. $h_2(x, y) = \bar{x}y \triangledown xy \triangledown x\bar{y}$ $[\langle \lambda^+, \lambda^+ \rangle \rightarrow \lambda^+ \triangledown \lambda^0 \triangledown \lambda^+]$. The soliton fusion is the keystone feature of the gate [38]. If the velocities of the bullets are below a certain threshold, the collided bullets do not overcome the binding forces and fuse into a single stationary soliton.

The formation of a stable stationary soliton may be used to build a counter in a light bullet universal computer. Namely, it allows us to organize the write operation. To read from the counter we should crash a light bullet into the stationary soliton. Unfortunately we do not know the possible outcomes of such collisions. Applying our experience with breathers, we can propose that depending on the velocity of the moving bullet and the degree of offset in the collision, there are several possible products of such a collision: (1) reflection of the moving bullet, (2) the setting of a previously stationary soliton into motion, or (3) the disappearance of the moving bullet.

9.3. Breathers

As defined in ref. 42, discrete breathers are the time-periodic, spatially localized solutions of equations of motion for classical degrees of freedom interacting on a lattice. The breather is a multisolition in the sense of the inverse scattering transformations [22, 23]. Flach *et al.* [41] obtained reliable numerical solution of discrete breathers in three-dimensional lattices and predicted a positive energy threshold for real-life three-dimensional lattices, e.g., dynamics of atoms in crystals. They demonstrated that breathers are generated on a lattice if the coupling is weak enough. Breather solutions have been calculated for conjugated polymers, polyacetelene, ionic crystals, and electric lattices; they can also be generated optically [42]. Actually, the mechanism of discreteness-induced energy localization works in a large variety of physical lattice systems [35]. Thus, e.g., considering a Hamiltonian with two variables describing transverse displacement of two bases belonging to the base pairs in the DNA molecule under different values of coupling constants between two nucleotides along the same strand, Forinash *et al.* [43, 44] showed that intrinsic local modes can be accidently formed due to the localization of thermal fluctuations and one of the mechanisms of their growth is the exchange of energy.

Many results have been obtained on effects of internal degrees of freedom on the mobility properties of localized excitations on nonlinear lattices [42]. Thus interactions between breathers and impurity modes may lead to the fusion of two breathers and the generation of a larger excitation [43, 44]. In the presence of an external potential, a discrete breather can be broken up into two spatially separate, coherent structures with individual motions [22,

23]. Finally, perturbation of the pinning mode in the anticontinuous limit gives us a method for constructing moving breathers with minimum shape alteration [26]. Unfortunately, there is still no rigorous proof of their motility [41, 42]. However, moving breathers with long lifetime can be found in numerical experiments [26, 28]. Thus Chen and Aubry [26] demonstrate that a breather moves as a classical particle in the presence of an appropriate perturbation.

When two breathers collide with each other, a new pattern is formed. This new pattern remains localized or generates two new breathers, depending on the perturbations and phase differences [26]. Bang and Peyrard [11] and Forinash *et al.* [43, 44] also report the survival of breathers after collisions and their energy exchange depending on phase differences. Thus, we have the following properties of breather collisions [43, 44, 35]:

1. The result of collision depends on the relative phases of breathers when they collide.
2. The energy exchange between two collided breathers is proportional to the difference of their amplitudes.
3. A large breather increases its energy as the result of collision; when two breathers collide with each other, only the breather with large amplitude remains recognizable, however, it loses some energy; if the amplitude of the larger breather increases, it means it collects some energy from the thermal fluctuations.
4. The larger breather is often set into motion by the collision.
5. Multiple collisions can prevent a weakly unstable breather from decaying.
6. If a breather grows in amplitude, the minimum energy barrier increases and this breather will be trapped by discreteness.
7. Local defects on the lattice, e.g., regions with different coupling constants, may cause breather reflection, temporary trapping, or even speedup, depending on the parameters.

Finding 4. The $g2$ and h_2 gates are realized in breather interactions. The breathers may survive collision or generate a new localized excitation, which in turn, forms two new breathers [26, 11, 43, 44]. Therefore the gate $g2$ is realizable. In ref. 26 it is found that the new pattern formed in the collision of two breathers can remain localized. It gives us an opportunity to construct an h_2 gate.

9.4. Exotic species

The members of this family are moderately investigated and no published results on the outcomes of real or numerically simulated interactions of

these species are known. The *fluctuons*, which are chains of short-lived pair creation-annihilation fermions [27], and *informions*, which arise from the self-interference of diffusional processes and are massless quanta of information [39], are abstract phenomena. So-called *worms*, or two-dimensional movable localizations observed in experiments with nematic liquid crystals, belong to the real physical world [33, 31, 32].

Liquid crystals have axial anisotropy (let it be the x-axis). There are four directions along which localized waves propagate [67]. A worm moves along the x-axis if not perturbed [67] and has a very distinctive shape. In the x-axis it rises steeply to its maximum at one end (head) and then decays gradually to another end (tail). The worm is narrow along the y-axis. The widths of the worms are more or less equal, whereas their lengths can vary significantly from exemplar to exemplar. No information about collisions between the worms is available. Fortunately, in some conditions the worm starts to move along the y-axis as well. It may be possible to turn the head of a worm during the motion. If so, worms can change their direction of movement as the result of collision. To make an analogy between worms in nematic crystals and ladders in the *Life without Death* model [48] we also note that worms usually grow, i.e., they become longer and longer in the process of evolution [67].

10. HOW TO SEARCH FOR DYNAMICAL COMPUTATION UNIVERSAL MODELS

There are several hints that allow us to detect the appropriate candidates in the real world. Thus, for discrete breathers we know at least two criteria that can be used in the experimental search: energy threshold and scattering of planar waves by breathers [42]. Viability of the first criterion is proved in numerical experiments with cellular automata models of excitable media [7]: self-localized excitation in the lattice appears in evolution when every cell of the lattice has subcritical threshold of excitation; increasing the threshold of the cell excitation leads the system from spatial particle-like wave solutions through quasi-chaotic regimes to regimes with unidirectional and spiral waves [7]. Another confirmation of the 'subcritical threshold' is presented in ref. 44: in one-component systems brathers exist only below a critical coupling. In investigations of spatially localized excitations in a lattice of coupled oscillators it was found that breather-like patterns are more typical for small coupling between oscillators, whereas large coupling leads to the globally chaotic state [1].

Jakubowski, Steiglitz, and Squier [52] offer a realistic guide for searching for physics-based computation universality. A possible computationally universal system should satisfy the following antagonistic requirements: (i) self-

localized waves must preserve their integrity after a sequence of collisions and (ii) self-localized waves must lose a negligible amount of energy through radiation [52]. Based on the results of numerical experiments with the cubic nonlinear Shrödinger equations Jakubowsky *et al.* [52] show that even simple measures of the radiation may be very suitable in practical evaluations of the usefulness of wave collisions. Following their results we can indicate possible candidates: Kerr materials, media with laser beam propagation, spatiotemporal photoreactive optical solitions, and optical solitons in some kinds of atomic crystals [52].

In the abstract cellular-automata models (without any realistic constraints) we can simply build an automaton with the required behavior. In this case we can use genetic algorithms (see, e.g., ref. 57), sculpture the basin attraction fields [81], reconstruct the local transition rules from given global configurations [3], and generate predetermined patterns using integer programming techniques [20].

Problem 3. Let $\mathfrak{A}$ be the d-dimensional, 3-state, closest-neighborhood cellular automata model of lattice excitation, the cells of which update their states by the rule

$$x^{t+1} = \begin{cases} + & x^t = . \quad \text{and} \quad \left|\{y \in u(x) : y^t = +\}\right| = \theta \\ - & x^t = + \\ . & \text{otherwise} \end{cases} \tag{2}$$

Is it true for any $d > 0$ that the $\mathfrak{A}$ is universal when $\theta = 2^{d-1}$.

This criterion of universality holds for $d = 2, 3$, as demonstrated in the present paper. It is also true for $d = 1$: we can use a one-dimensional lattice to realize the $x \wedge \bar{y}$ gate if we launch the waves of the excitation on the tops of the lattice. For $d > 3$ the answer is still uncertain.

APPENDIX

Here we present explicit parameters of the elementary particles just a few steps before the collision. Assuming an entirely-rest three-dimensional lattice, we describe every collision by the sets $\mathbb{C}_+$ and $\mathbb{C}_-$ of the coordinates of cells being in rest (+) and refractory (−) states, respectively. The coordinates are represented relative to the (0, 0, 0) coordinate center placed in the (n/2, n/2, n/2) cell of the three-dimensional lattice.

The frontal collision of two 6^+-particles with the formation of stationary gun:

$\mathbb{C}_+ = \{(12, 10, 0), (12, 11, 0), (10, 12, 0), (12, 10, 1), (12, 11, 1), (10, 12, 1), (0, 0, 0), (0, 0, 1), (0, 1, 0), (0, 1, 1,), (2, -1, 0), (2, -1, 1)\}$

$\mathbb{C}_- = \{(11, 11, 0), (13, 11, 0), (11, 13, 0), (11, 11, 1), (13, 11, 1), (11, 13, 1), (-1, 0, 0), (-1, 0, 1), (1, 0, 0), (1, 0, 1), (1, -2, 0), (1, -2, 1)\}$

The coordinates of 4^+- and 6^+-particles in the $h2$ gate:

$\mathbb{C}_+ = (0, 0, 0), (0, 0, 1), (0, 1, 0), (0, 1, 1), (2, -1, 0), (2, -1, 1), (0, -9, 0), (1, -9, 0), (0, -9, 1), (1, -9, 1)$

$\mathbb{C}_- = (-1, 0, 0), (-1, 0, 1), (1, 0, 0), (1, 0, 1), (1, -2, 0), (1, -2, 1), (0, -10, 0), (1, -10, 0), (0, 10, 1), (1, -10, 1)$

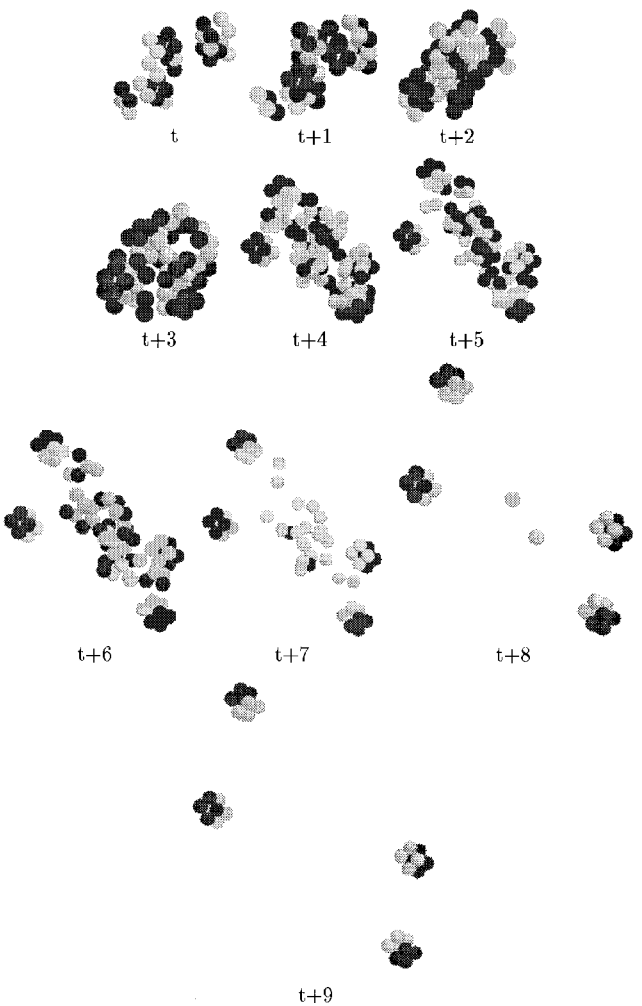

Fig. 27. Collision of three 6^+–particles with the formation of four 4^+–particles in the $h6$–gate.

The coordinates of 4^+- and 6^+-particles in the $h4$ gate:

$\mathbb{C}_+ = (0, 0, 0), (0, 0, 1), (0, 1, 0), (0, 1, 1), (2, -1, 0), (2, -1, 1), (0, -5, 0), (1, -5, 0), (0, -5, 1), (1, -5, 1)$

$\mathbb{C}_- = (-1, 0, 0), (-1, 0, 1), (1, 0, 0), (1, 0, 1), (1, -2, 0), (1, -2, 1), (0, -6, 0), (1, -6, 0), (0, -6, 1), (1, -6, 1)$

The coordinate of three 6^+-particles colliding in $h6$-gates (the full history of the collision is shown in Fig. 27):

$\mathbb{C}_+ = (0, 0, 0), (0, 0, 1), (0, 1, 0), (0, 1, 1), (2, -1, 0), (2, -1, 1), (1, 5, 0), (1, 6, 0), (3, 7, 0), (1, 5, 1), (1, 6, 1), (3, 7, 1), (4, 1, 0), (4, 2, 0), (2, 3, 0), (4, 1, 1), (4, 2, 1), (2, 3, 1)$

$\mathbb{C}_- = (-1, 0, 0), (-1, 0, 1), (1, 0, 0), (1, 0, 1), (1, -2, 0), (1, -2, 1), (0, 6, 0), (2, 6, 0), (2, 8, 0), (0, 6, 1), (2, 6, 1), (2, 8, 1), (3, 2, 0), (5, 2, 0), (3, 4, 0), (3, 2, 0), (5, 2, 1), (3, 4, 1)$

REFERENCES

[1] M. Abel and A. Pikovsky, Parametric excitation of breathers in a nonlinear lattice. *Z. Naturforsch. A. J. Phys. Sci.* **52** (1997), 570–572.

[2] M. J. Ablowitz, J. M. Keiser, and L. A. Takhtajan, Class of stable multistate time- reversible cellular automata with rich particle content, *Phys. Rev. A* **44** (1991), 6909–6912.

[3] A. Adamatzky, *Identification of Cellular Automata* (Taylor and Francis, London, 1994).

[4] A. Adamatzky, Controllable transmission of information in excitable media: The 2^+-media, *Adv. Mater. Opt. Electron.* **5** (1995), 145–155.

[5] A. Adamatzky, On the particle like waves in the discrete model of excitable medium, *Neural Netw. World* **1** (1996), 3–10.

[6] A. Adamatzky, Universal computation in excitable media: The 2^+-media, *Adv. Mater. Opt. Electron.* **7** (1997), 263–272.

[7] A. Adamatzky and O. Holland, Parameterisation of the local excitation of 2D lattices: morphology, dynamics and computation, Unpublished (1998).

[8] K. Agladze, N. Magome, R. Aliev, T. Yamaguchi, and K. Yoshikawa. Finding the optimal path with the aid of chemical wave, *Physica D* **106** (1997), 247–254.

[9] R. Anderson, L. Lovász, P. Shor, J. Spencer, E. Tardós, and S. Winograd, Disks, balls and walls: Analysis of a combinatorial game, *Am. Math. Mont.* **96** (1989), 481–493.

[10] P. Bak, C. Tang, and K. Wiesenfeld, Self-organized criticality. *Phys. Rev. A* **38** (1988), 364–374.

[11] O. Bang and M. Peyrard, Generation of high-energy localized vibrational modes in nonlinear Klein–Gordon lattices, *Phys. Rev. E* **53** (1996), 41–43.

[12] E. R. Banks, Information and transmission in cellular automata, *Ph.D. Diss.*, MIT, (1971).

[13] C. Bays, A new game of three-dimensional Life, *Complex Syst.* **5** (1991), 15–18.

[14] C. H. Bennett, Universal computation and physical dynamics, *Physica D* **86** (1995), 268–273.

[15] E. Berlekamp, J. Conway, and R. Guy, *Winning Ways*, Vol. **2** (Academic Press, New York, 1982).

[16] J. Bitar and E. Goles, Parallel chip firing games on graphs, *Theor. Comput. Sci.* **92**, (1992), 291–300.

[17] A. B. Blagoeva, S. G. Dinev, A. A. Dreischuh, and A. Naidenov, Light bullets formation in a bulk media, *IEEE J. Quantum Electronics* **27** (1991), 2060.
[18] R. Blittersdorf, J. Miller, and F. W. Schneider, Chemical visualization of Boolean functions: A simple chemical computer, *J. Chem. Educ.* **72** (1995), 760–763.
[19] A. Bobenko, M. Bordemann, C. Gunn, and U. Pinkall, On 2 integrable cellular-automata, *Commun. Math. Phys.* **158** (1993), 127–134.
[20] R. A. Bosch, Using integer programming to find still lifes and oscillators in Conway's game of Life, Unbpulished (1998).
[21] M. S. Branicky, Universal computation and other capabilities of hybrid and continuous dynamical systems, *Theor. Comput. Sci.* **138** (1995), 67–100.
[22] D. Cai, A. R. Bishop, and N. Gronbechjensen, Spatially localized, temporally quasi-periodic, discrete nonlinear excitations. *Phys. Rev. E* **52** (1995), 5784–5787.
[23] D. Cai, A. R. Bishop, and N. Gronbechjensen, Discrete lattice effects on breathers in a spatially linear potential, *Phys. Rev. E* **53** (1996), 1202–1205.
[24] H. Chang, Magnetic-bubble conservative logic, *Int. J. Theor. Phys.* **21** (1982), 955–960.
[25] H. F. Chau and F. Wilczek, Simple realization of the Fredkin gate using a series of 2-body operators, *Phys. Rev. Lett.* **75** (1995), 748–750.
[26] D. Chen, S. Aubry, and G. P. Tsironis, Breather mobility in discrete Ψ^4 nonlinear lattices, *Phys. Rev. Lett.* **77** (1996), 4776–4779.
[27] M. Conrad, Fluctuons I. Operational analysis, *Chaos, solitons Fractals* **3** (1993), 411–424.
[28] P. L. Christiansen, Yu. B. Gaididei, V. K. Mezentsev, S. L. Musher, K. O. Rasmussen, J. Juul Rasmussen, I. V. Ryzhenkova, and S. K. Turitsyn, Discrete localized states and localization dynamics in discrete nonlinear Schrödinger equations, *Physica Scripta T* **67** (1996), 160–166.
[29] J. Dassow and H. Jurgensen, Soliton automata, *Lect. Notes Comput. Sci.* **278** (1987), 95–102.
[30] J. Dassow and H. Jurgensen, Deterministic soliton automata with a single exterior node, *Theor. Comput. Sci.* **84** (1991), 281–292.
[31] M. Dennin, G. Ahlers, and D. S. Cannell, Chaotic localized states near the onset of electroconvection, *Phys. Rev. Lett.* **77** (1996), 2475–2478.
[32] M. Dennin, G. Ahlers, and D. S. Cannell, Spatiotemporal chaos in electroconvection, *Science* **272** (1996), 388–390.
[33] M. Dennin, D. S. Cannell, and G. Ahlers, Patterns of electroconvection in a nematic liquid crystal, *Phys. Rev. E* **57** (1998), 638–649.
[34] J. Durand-Lose, About the universality of the billiard ball model, In *Proceedings Colloqium Mathematical Machines and Computation, Metz* (1998).
[35] T. Duxois and M. Peyrard, Energy localization in nonlinear lattices, *Phys. Rev. Lett.* **25** (1993), 3935–3938.
[36] D. E. Edmundson and R. H. Enns, Fully 3-dimensional collisions of bistable light bullets, *Optics Lett.* **18** (1993), 1609.
[37] D. E. Edmundson and R. H. Enns, The particle-like nature of colliding light bullets, *Phys. Rev. A* **51** (1995), 2491–2498.
[38] D. Edmundson and R. Enns, *Light Bullet Home Page,* March 1996, http://www.sfu.ca/~renns/lbullets.html.
[39] M. S. El Naschie, A note on quantum mechanics, diffusional interference and informions, *Chaos, Solitons Fractals* **5** (1995), 881–884.
[40] P. C. Fisher, Generation of primes by a one-dimensional real-time interative arrays, *J. ACM* **12** (1965), 388–394.
[41] S. Flach, K. Kladko, and R. S. MacKay, Energy thresholds for discrete breathers in one-, two-, and three-dimensional lattices, *Phys. Rev. Lett.* **78** (1997), 1207–1210.

[42] S. Flach and C. R. Willis, Discrete breathers, *Physica Rep.* (1997).
[43] K. Forinash, M. Peyrard, and B. Malomed, Interaction of discrete breathers with impurity modes, *Phys. Rev. E* **49** (1990), 3400–3411.
[44] K. Forinash, T. Cretegny, and M. Peyrard, Local modes and localization in a multicomponent nonlinear lattices, *Phys. Rev.* **55** (1997), 4740–4756.
[45] E. Fredkin and T. Toffoli, Conservative logic, *In. J. Theor. Phys.* **21** (1982), 219–253.
[46] B. Fuchassteiner, Filter automata admitting oscillating carrier waves, *Appl. Math. Lett.* **4** (1991), 23–26.
[47] M. Gardner, *Wheels, Life and Other Mathematical Amusements* (Freeman, New York, 1983).
[48] D. Griffeath and C. Moore, Life without death is *P*-complete; www.santafe.edu/~Moore (1997).
[49] E. Goles and M. Margenstern, Sand pile as a universal computer, *Int. J. Mod. Phys.* **7** (1996), 113–122.
[50] E. Goles and M. Kiwi, Games on linear graphs and sand piles, *Theor. Comput. Sci.* **115** (1993), 321–349.
[51] E. Goles and M. Matamala, Reaction-diffusion automata: Three states implies universality, *Theory Comput. Sys.* **30** (1997), 223–229.
[52] M. H. Jakubowski, K. Steiglitz, and R. Squier, Information transfer between solitary waves in the saturable Schrödinger equation, *Phys. Rev. E* **56** (1997), 7267–7272.
[53] P. Koiran, M. Cosnard, and M. Garzon, Computability with low-dimensional dynamical systems. *Theor. Comput. Sci.* **132** (1994), 113–128.
[54] L. Kuhnert, Photochemische Manipulation von chemischen Wellen, *Naturwissenschaften* **2** (1986), 96–97.
[55] L. Kuhnert, K. L. Agladze, and V. I. Krinsky, Image processing using light-sensitive chemical waves, *Nature* **337** (1989), 244–247.
[56] J. Mazoyer, Computations on one-dimensional cellular-automata, *Ann. Math. Artific. Intell.* **16** (1996), 285–309.
[57] M. Mitchell, Computation in cellular automata: A selected review, *Santa Fe Institute Working Paper* **96-09-074** (1996).
[58] K. Morita and S. Ueno, Computation universal model of 2D 16-state reversible partitioned cellular automaton, *IEICE Trans. Inf. Syst.* **E75-D** (1992), 141–147.
[59] K. Nakamura, Parallel universal simulation and self-reproduction in cellular spaces, *IEICE Trans. Inform. Syst.* **E80D** (1997), 547–552.
[60] S. Omohundro, Modelling cellular automata with partial differential equations, *Physica D* **10** (1984), 128–134.
[61] P. Orponen and M. Matamala, Universal computation by finite two-dimensional coupled map lattices, In *PhysComp96: Proc. Workshop on Physics and Computation*, extended abstract (1996).
[62] J. K. Park, K. Steiglitz, and W. P. Thurston, Soliton-like behaviour in automata, *Physica D* **19** (1986), 423–432.
[63] T. S. Papatheodorou, M. J. Ablowitz, and Y. G. Saridakis, A rule for fast computation and analysis of soliton automata, *Stud. Appl. Math.* **79** (1988), 173–184.
[64] N. G. Rambidi and A. V. Maximichev, Molecular image-processing devices based on chemical reaction systems. 3: Some operational characteristics of excitable light-sensitive media used for image processing, *Adv. Mater. Opt. Electron.* **5** (1995), 223–231.
[65] N. G. Rambidi and A. V. Maximichev, Molecular image-processing devices on chemical reaction systems. 6. Processing half-tone images and neural network architecture of excitable media, *Adv. Mat. Optics Electr.* **7** (1997), 171–182.

[66] N. Reimen and J. A. Mazoyer, Linear speed-up theorem for cellular automata, *Theor. Comput. Sci.* **101** (1992), 59–98.
[67] H. Riecke and G. D. Granzow, Localization of waves without bistability: Worms in nematic electroconvection (1998).
[68] H. T. Siegelman, The simple dynamics of super Turing theories, *Theor. Comput. Sci.* **168** (1996), 461–472.
[69] H. T. Siegelman and E. D. Sontag, Analog computation via neural networks, *Theor. Comput. Sci.* **131** (1994), 331–360.
[70] R. K. Squier and K. Steiglitz, 2D FHP lattice-gases are computation universal, *Complex Syst.* **7**, (1993) 297–307.
[71] R. K. Squier, K. Steiglitz, and M. H. Jakubowski, State transformations of colliding optical solitons and possible application to computation in bulk media, *Phys. Rev. E* **58** (1998), 6752–6758.
[72] R. K. Squier and K. Steiglitz, Programmable parallel arithmetic in cellular automata using a particle model, *Complex Syst.* **8** (1994), 311–323.
[73] R. K. Squier, K. Steiglitz, and M. H. Jakubowski, Implementation of parallel arithmetic in a cellular automaton, In *Proc. 1995 Int. Conf. on Application Specific Array Processors,* Strasbourg, 1995.
[74] K. Steiglitz, I. Kamal, and A. Watson, Embedded computation in one-dimensional automata by phase coding solitons, *IEEE Trans. Comp.* **37** (1988), 138–145.
[75] O. Steinbock, A. Tóth, and K. Showalter, Navigating complex labyrinths: Optimal paths form chemical waves, *Science* **267** (1995), 868–871.
[76] O. Steinbock, P. Kettunen, and K. Showalter, Chemical wave logic gates, *J. Phys. Chem.* **100** (1996), 18970–18975.
[77] D. Takahashi and J. Matsukidaira, On discrete soliton-equations related to cellular-automata, *Phys. Lett. A* **209** (1995), 184–188.
[78] T. Tokihiro, D. Takahashi, J. Mattsukidaira, and J. Satsuma, From soliton-equations to integrable cellular-automata through a limiting procedure, *Phys. Rev. Lett.* **76** (1996), 191–196.
[79] D. Tolmachev and A. Adamatzky, Chemical processor for computation of Voronoi diagram, *Adv. Mater. Opt. Electron.* **6** (1996), 191–196.
[80] Á. Tóth and K. Showalter, Logical gates in excitable media, *J. Phys. Chem.* **103** (1995), 2058–2066.
[81] A. Wuensche and M. Lesser, *The Global Dynamics of Cellular Automata* (Addison-Wesley, Reading, Massachusetts, 1992).